Modelling unusual X-ray emission from wind-driven black hole binary Cyg X-3 with AstroSat.

Jarupula Gopal

Email:ep18btech11004@iith.ac.in

Supervisor : Mayukh pahari

Email:mayukh@phy.iith.ac.in

INTRODUCTION:

Establishing the true nature of the connection between the accretion disk and radio jets in X-ray binaries at different mass accretion rates has been considered one of the challenging problems in astrophysics and several attempts have been made so far in this direction . Such attempts successfully establish the long-term radio/X-ray correlations from weeks to years timescales in both transient and persistent/semi-persistent sources like GX 339-4 ,Cyg X-1 , GRS 1915+105, and Cyg X-3. However, there are a handful of attempts where inner disk activity was closely monitored before, during, and after the superluminal radio ejection from X-ray transients.

Until now, the changes in X-ray spectro-temporal properties during the formation of a superluminal jet have been monitored with the frequency of days to weeks, except GRS 1915+105, which is the only source that has radio and sensitive X-ray data on a scale of days. However, depending upon the size of the radio jet base, it is possible that the decoupling may occur in the first few minutes to hours and may leave a signature in X-ray spectro-timing properties. Unfortunately, no studies exist where the change in X-ray properties of the inner accretion flow are traced with the accuracy of a timescale of minutes. One key reason for the lack of such studies is that superluminal radio ejections are rare, transient, and their time of occurrences are completely unpredictable within a timescale of days to weeks. Therefore, it is difficult to determine the time of radio jet formation more accurately than a few days.

Due to high X-ray and radio fluxes, Cyg X-3 is a potential X-ray source for such studies. In this work, we analyze the simultaneous observations of Cyg X-3 using the Soft X-ray Telescope(SXT) and Large Area X-ray Proportional Counter (LAXPC) instruments on boardAstroSat.

In this work, we analyze the simultaneous observations of Cyg X-3 using the Soft X-ray Telescope (SXT) and Large Area X-ray Proportional Counter (LAXPC) instruments on board AstroSat. Based on light curve, hardness, and broadband energy spectra, we found that during the first 10–12 hr, the source was in the HPS. After ~50 ks, an unusual, flat power-law component appeared in the spectrum of Cyg X-3, and we termed it as the very high state (VHS). We show that the flat power-law component is consistent with the synchrotron emission from the radio jet monitored simultaneously with the RATAN telescope. This observation provides an opportunity to closely monitor the X-ray properties during the formation of giant radio flares in Cyg X-3.

What is Cygnus X-3 (Cyg x-3)?

1. Cyg X-3 is a Galactic X-ray binary, with a high mass companion and accreting via wind from the equatorial plane of the companion star.

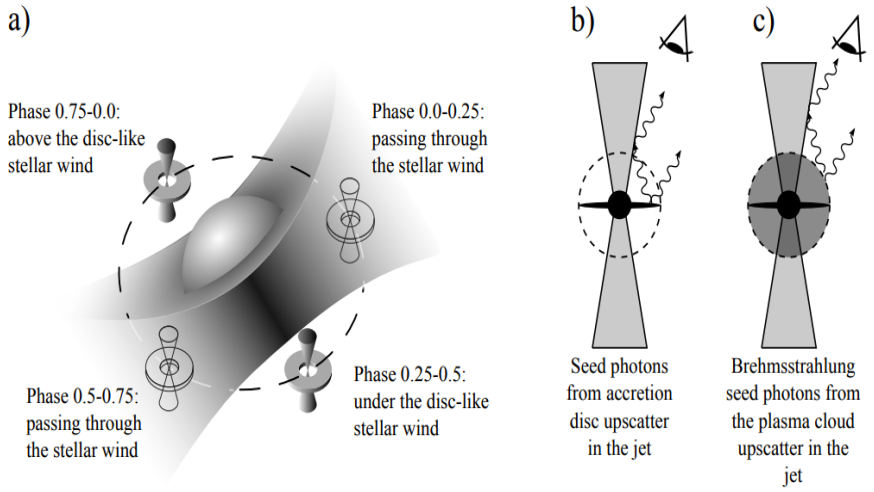

2.It is the brightest Radio source (~ 10 Jy) during its jet emission and emits photons until TeV range

3. Strong correlated variability between X-ray intensity and Radio jets have been observed over a long time scale

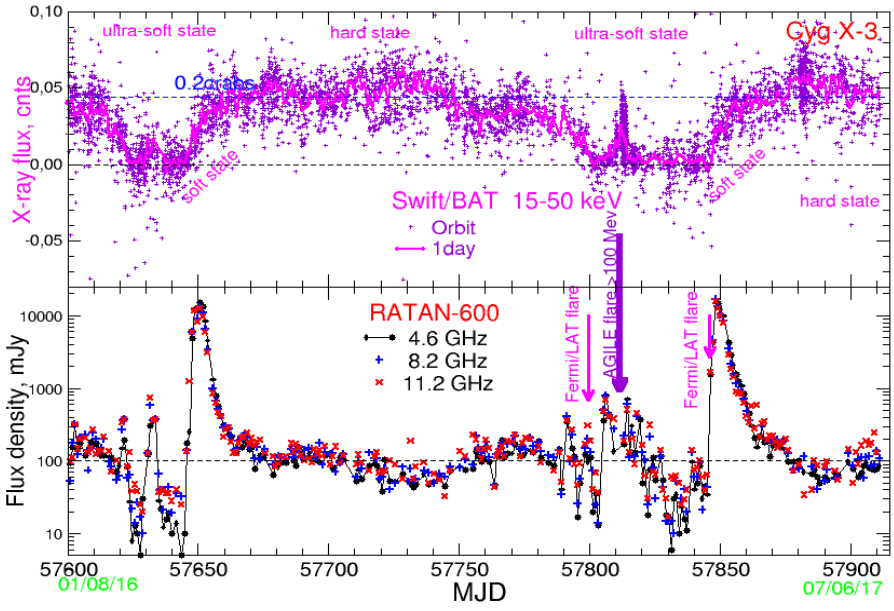

:The top one is the x-ray flux which changes from 15-50 kev. And the bottom one is the radio flux .

The correlation is that when the x-ray flux goes down then typically it is fine, but when it rises then radio flares occur .which is typically 10jy. And we have to notice that this pattern is happening repeatedly .....notice here that when x-ray flux is close to zero..after some time it started rising ..at that time radio flares occur..this is the facility of the source and they are well correlated .

An important tool in understanding the nature of the transient black hole systems is the hardness-intensity diagram . Thus it should be natural to look at Cyg X-3's HID and compare it to other black hole systems, all the while bearing in mind that Cyg X-3 does not behave like a transient black hole XRB in outburst. Nevertheless, we find the HID to be a useful tool even in this case.

Motivations:

There are lots of x-ray spectra and HID studies of cygnus x-3 is done.

1.X-ray spectral study and modelling is important to understand the underlying physical processes (both thermal and non-thermal emissions) and the geometry of the accreting system (predicted from spectral parameters).

2.A typical black hole HID representing the transient outbursting cycle has a Q-type shape that can be divided into four main areas or states: quiescent, low/hard (LH), very high/intermediate (VHS/IS) and high/soft (HS) state.

THE HARDNESS-INTENSITY DIAGRAM (HID) OF CYGNUS X-3:

Figure shows the HID for Cyg X-3. The bands were chosen so as to probe different emission regions, with the SXR (3– 6 keV) range representing the disc and HXR (10–15 keV) range representing the Comptonized part of the spectrum.The harder band was chosen in this study to ensure that the disc (1.3–1.6 keV in the HS state) does not significantly contribute to it.

At first glance the plot appears surprisingly similar to other black hole XRB HIDs, but there are some very important differences. First of all, Cyg X-3 does not show hysteresis in the HID (Hjalmarsdotter et al. 2009) but simply increases in intensity as the spectrum softens (maximum RXTE/PCA intensity 1200 counts/s/PCU or ~ 1 × 10−8 erg/cm2 /s in the 3–15 keV band, in the flaring/hypersoft states as compared to 200 counts/s/PCU or ~ 2 × 10−9 erg/cm2 /s in the quiescent state). In black hole XRBs the LH state is present throughout the right branch, whereas in Cyg X-3 the LH state is confined to the foot of the Q. The right branch in this case is dominated by Xray flaring in Cyg X-3. In addition, the flaring data are also spread into different hardnesses which wholly fill the inside area of the Q.

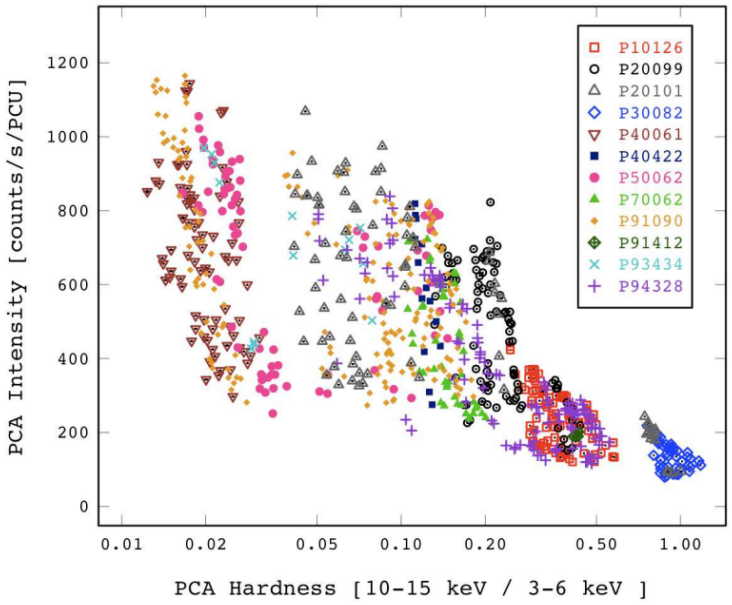

> Variability in Cygnus X-3's HID:

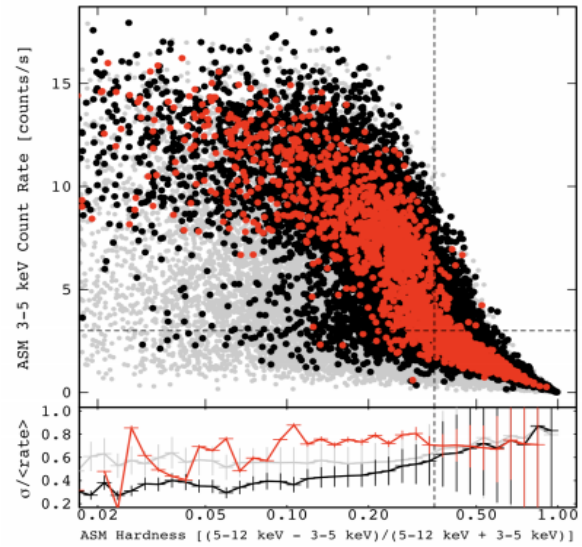

As we see in the Cyg X-3 HID, there is a noticeable scatter present in the intensity for each value of hardness and the most striking transition happens when the system moves in or out of the flaring region. A vertical line in Fig marks the change in the system from the LH state to the HS state or vice versa, and we see a corresponding increase/decrease in SXR flux . The scatter in the intensity is partly due to the strong orbital motion detected in the system which affects the intensity approximately by a factor of two. The orbital modulation impacts also on the hardness ratios). On top of that we expect X-ray flaring occurring in the system which will increase the variability in the intensity by some amount.

Classifications of Cygnus X-3's Radio/X-ray spectral States:

In Figure, the HID for Cyg X-3 is plotted using a new approach: the data points with (near-)simultaneous radio coverage have been coloured according to the strength of the radio flux density (data from Table 1), with darker points representing a weaker radio source and lighter points a brighter radio source.

Table 1. Different classification methods of Cyg X-3 X-ray spectra with corresponding radio activity.

Canonical X-ray states	Radio states[a]	X-ray states of S04[b]		radio/X-ray states of S08[c]	This paper
		group:	name:		
low/hard	quiescent	1	hard	quiescent	quiescent
		2	intermediate	minor flaring	transition
intermediate	minor flaring	3	very high	suppressed "post-flare"	FHXR
high/soft	major flaring	4	soft non-thermal	major flaring	FIM
	quenched	5	ultrasoft	quenched	FSXR hypersoft

Thus the radio/X-ray states are clearly revealed in the HID and we divide them according to the X-ray hardness and/or radio flux into three distinct areas that we call hypersoft, flaring and quiescent.

In addition,the flaring state can be further subdivided according to X-ray hardness and the shape of the spectra: flaring/soft X-ray (FSXR), flaring/intermediate (FIM) and flaring/hard X-ray (FHXR).. The quiescent state can also be subdivided into two regions: quiescent and transition.

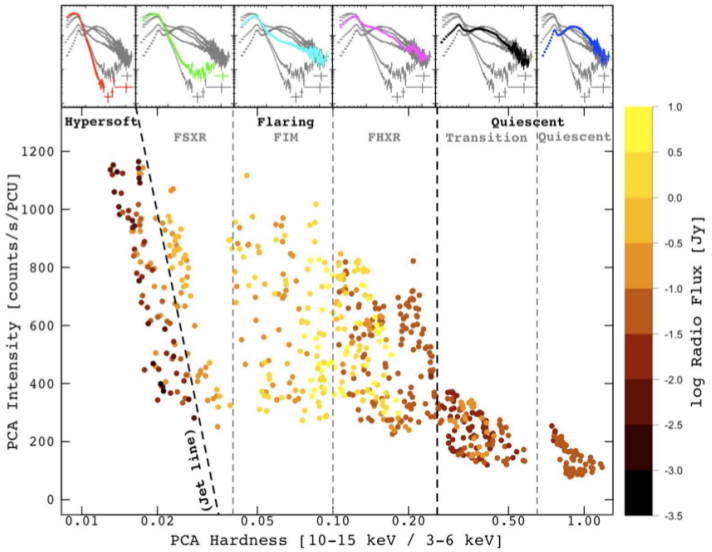

The above figure is divided into six different areas which correspond to six different X-ray states of Cyg X-3.based on the hardness and the intensity.

Quiescent State :The quiescent region comprises the lower right corner of the HID, bounded by the flaring region on the left side.cyg X-3 is found to spend ~ 52 % of the time in the quiescent states and the rest in the flaring states.
Transition State:. In the transition region the radio flux starts to increase and the power law component of the spectrum starts to flatten shifting the HXR spectral peak towards softer energies, i.e. the X-ray hardness decreases and the source moves to the left in the HID.
Flaring/Hard X-ray State (FHXR) : It is bound by the transition region on the right side and the hypersoft region on the left side. The most striking aspect of the flaring states is the increased radio and X-ray emission which corresponds to the canonical spectral change from the LH to the HS state when the intensity of the soft component increases
Flaring/Intermediate State (FIM) :This state lies between the areas of FHXR and FSXR in the HID and is characterized by major flaring. The X-ray spectrum is similar to the FHXR spectrum with slightly less contribution to the HXR . The FIM and FHXR are the states in which Cyg X-3 mainly alternates right after a major flare event.

Flaring/Soft X-ray State (FSXR): the FSXR state and the hypersoft state. The spectrum of the FSXR state is soft without significant HXR emission. However, it shows a weak power law tail extending to higher energies.
The line that demarcates these two states is the so-called **jet line** and most remarkably, unlike transient black hole XRBs, Cyg X-3 crosses this line from right to left (from FSXR to hypersoft) with- out producing a major radio flare. It is only when it crosses from left to right that a major flare occurs.
Hypersoft state:the radio emission falls to very low values, the HXR vanishes, and thus the HXR and radio switch from an anti-correlation to a correlation. In this state, the radio flux is well below and the SXR is above the transition level, and it is after Cyg X-3 emerges from this state that a major radio flare occurs.

The X-ray spectra of Cyg X-3 are notoriously complex. Cyg X-3 exhibits the canonical X-ray states seen in other XRBs, namely the high/soft (HS) and low/hard (LH) states, in addition to the intermediate, very high and ultrasoft states which have very different spectral shapes.

The spectra for all states are shown in Figure:

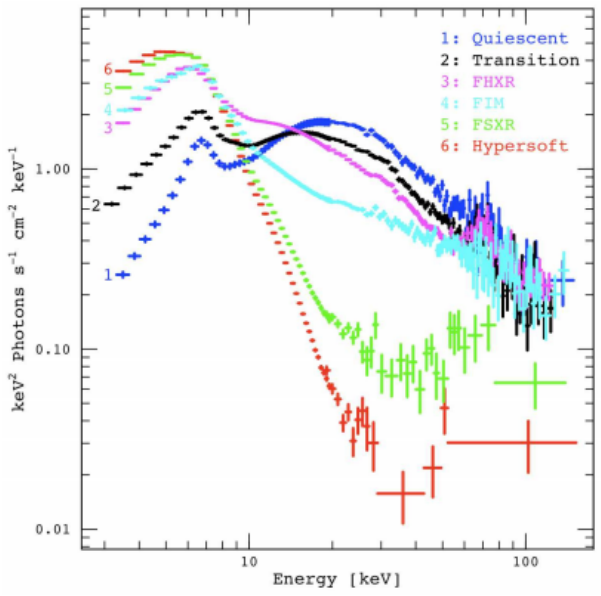

>Many attempts to understand Cyg X-3 spectral properties failed due to incomplete spectral data .Therefore, we attempted broadband spectral modelling using **AstroSat**.Which consist of both soft and hard spectra.

What is ASTROSAT?

ASTROSAT observes the universe in the optical, Ultraviolet, low and high energy X-ray regions of the electromagnetic spectrum, whereas most other scientific satellites are capable of observing a narrow range of wavelength bands.

The objectives of the AstroSat mission are to design, develop, realize and launch a multi-wavelength astronomy satellite for studying the cosmic sources simultaneously over a wide **range** of the electromagnetic spectrum i.e from optical, ultraviolet (UV) to high energy X-rays.

Astrosat performs multi-wavelength observations covering spectral bands from radio, optical, IR, UV, and X-ray wavelengths. Both individual studies of specific sources of interest and surveys are undertaken. While radio, optical, and IR observations would be coordinated through ground-based telescopes, the high energy regions, i.eUV, X-ray and visible wavelength, would be covered by the dedicated satellite-borne instrumentation of *Astrosat.*

The scientific objectives of ASTROSAT mission are:

- To understand high energy processes in binary star systems containing neutron stars and black holes
- Estimate magnetic fields of neutron stars
- Study star birth regions and high energy processes in star systems lying beyond our galaxy
- Detect new briefly bright X-ray sources in the sky
- Perform a limited deep field survey of the Universe in the Ultraviolet region

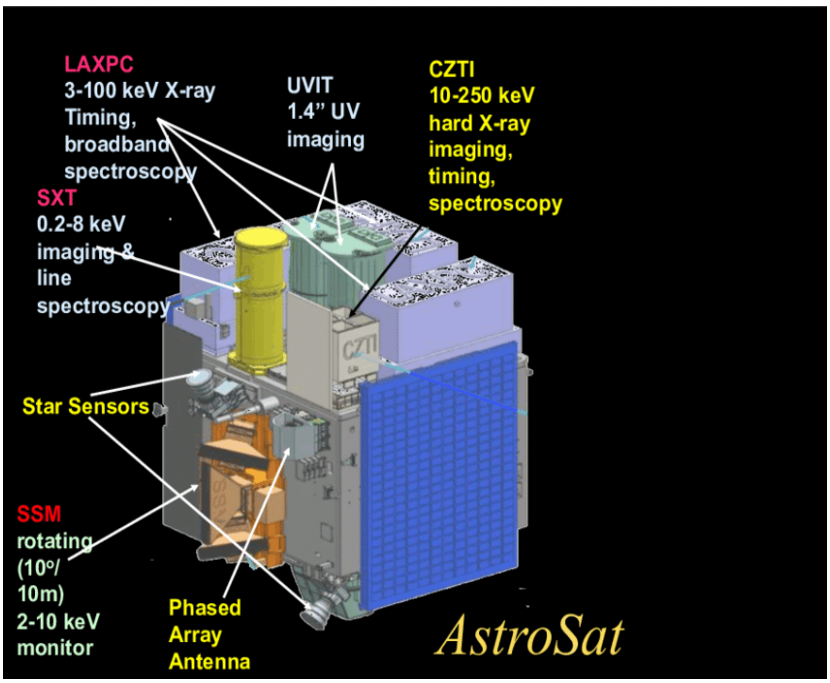

Payloads of ASTROSAT :

Five payloads of ASTROSAT are chosen to facilitate a deeper insight into the various astrophysical processes occurring in the various types of astronomical objects constituting our universe. These payloads rely on the visible, Ultraviolet and X-rays

coming from distant celestial sources.

1. The Ultraviolet Imaging Telescope (UVIT), capable of observing the sky in the Visible, Near Ultraviolet and Far Ultraviolet regions of the electromagnetic spectrum
2. Large Area X-ray Proportional Counter (LAXPC), is designed for studying the variations in the emission of X-rays from sources like X-ray binaries, Active Galactic Nuclei and other cosmic sources.
3. Soft X-ray Telescope (SXT) is designed for studying how the X-ray spectrum of 0.3-8 keV range coming from distant celestial bodies varies with time.
4. Cadmium Zinc Telluride Imager (CZTI), functioning in the X-ray region, extends the capability of the satellite to sense X-rays of high energy in the 10-100 keV range.
5. Scanning Sky Monitor(SSM), is intended to scan the sky for long term monitoring of bright X-ray sources in binary stars, and for the detection and location of sources that become bright in X-rays for a short duration of time.

In this work,We have used X-ray spectra obtained from Indian multiwavelength astronomical mission AstroSat.and only two payloads **SXT and LAXPC.**

Observations and Analysis :

For broadband spectroscopic purposes, we use simulation observations from the SXT and LAXPC instruments.

SXT is a focusing telescope with a CCD camera that can perform X-ray imaging and spectroscopy in the 0.3–8.0 keV energy range. Level 1 imaging mode data are processed through a pipeline software to produce level 2 event files and then a good time interval corrector and SXT event merger script is used to create merged event files from all the clean events with the corrected exposure time. We use XSELECT V2.4d in HEASOFT 6.22.1 to extract light curves and spectra using source regions between 1 and 13 arcmin. An off-axis auxiliary response file (ARF) appropriate for the source location on the CCD is generated from the provided on-axis ARF using sxtmkarf tool (see footnote 9). Blanksky SXT observations are used to extract background spectrum.

LAXPC consists of three identical X-ray proportional counters with the absolute time resolution of 10 μs in the energy range 3.0–80.0 keV. LAXPC data is analyzed using the LAXPC software.

In the below figure ,we show the Swift/BAT daily light curve in 15–50 keV where the AstroSat observation span is marked by two vertical lines. The light curve shows that the Swift/BAT count rate sharply rises by a factor of ~2 within the AstroSat observation period. The bottom panel shows the 11.2 GHz radio light curve obtained from the RATAN-600 telescope (Trushkin et al. 2017a). The radio flux density was at a low, persistent level of ~50–100 mJy until MJD 57845 and then it rose to ~1 Jy within the AstroSat observation window. Therefore, the AstroSat observation during the onset of the giant radio flare simultaneous with the X-ray hardening is extremely valuable to monitor the disk/jet connections.

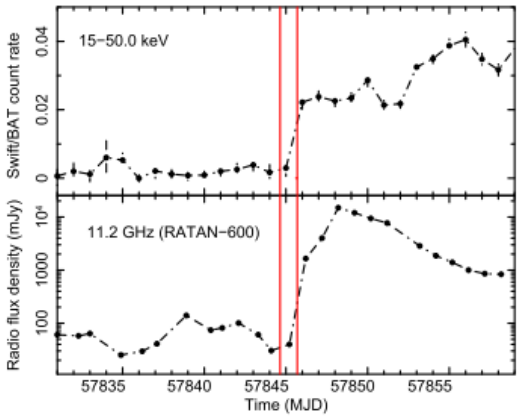

The 3–80 keV background-subtracted LAXPC light curve and 0.3–8 keV SXT light curve are shown in the Figure. We note that the peak count rate of the binary modulation of ~4.8 hr observed from both LAXPC and SXT light curves increases significantly (~50%) after ~60 ks.

To check the soft and hard X-ray behavior of the source, we plot the 3–10 keV, 17–60 keV background subtracted light curves and their ratios in the Figure .

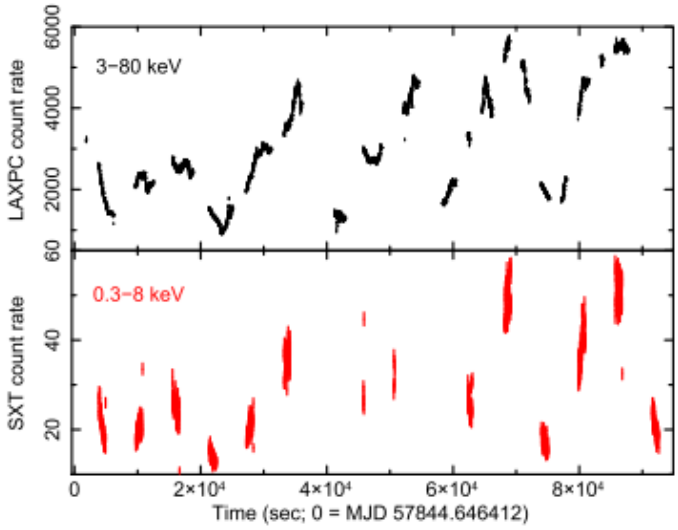

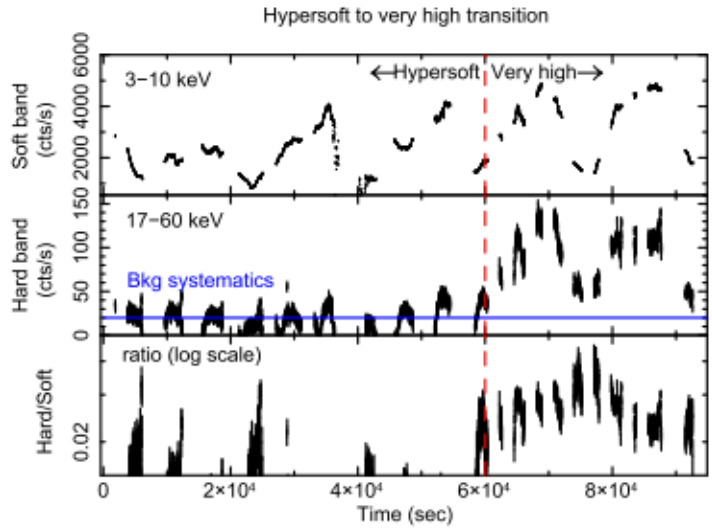

The hard component appears from 60 ks onward during VHS. We check the flux–flux plot in 3–6 keV and 15–60 keV using LAXPC10 observations shown in Figure.

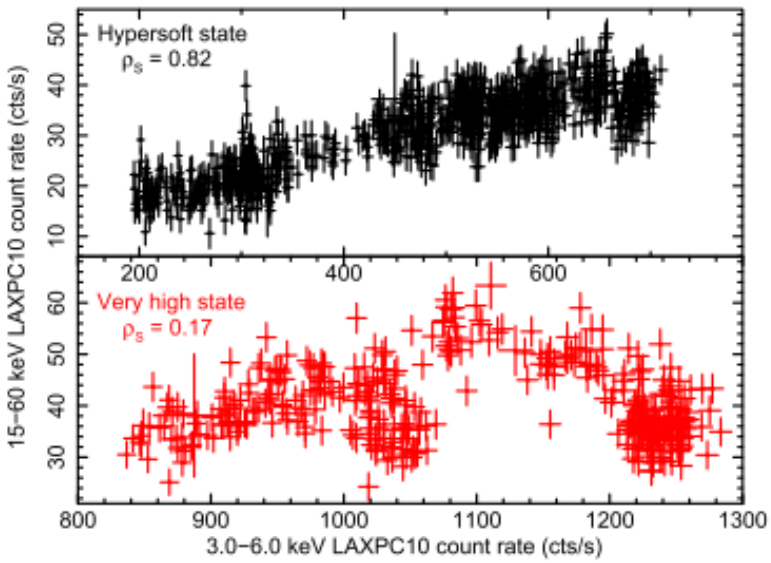

>During the HPS, the 3–6 keV count rate strongly correlates with the 15–60 keV count rate with the Spearman rank correlation coefficient (SRCC) of 0.82 (two-tailed p-value is <0.0000004), while both light curves are not correlated during the VHS with the SRCC of 0.17 (two-tailed p-value is ~0.0006). The non-correlation indicates that the origin of hard and soft X-ray emission during the VHS may be independent of each other.

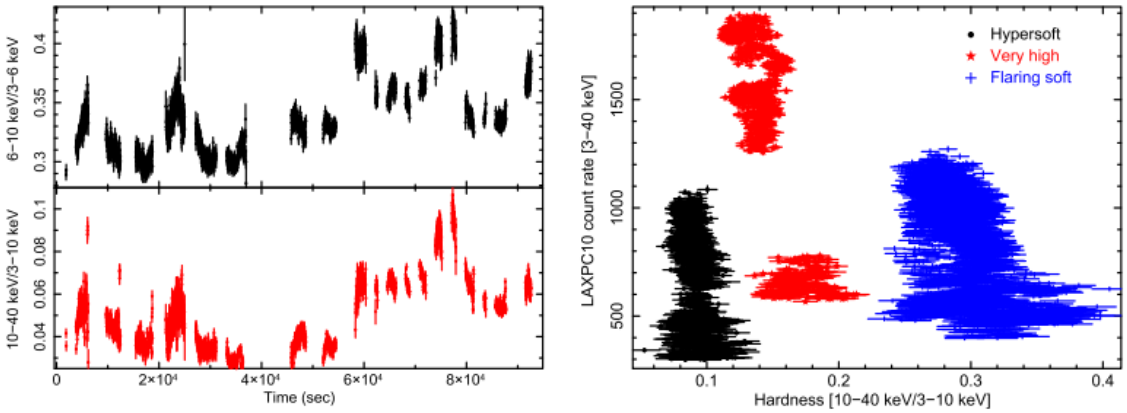

> Top left and bottom left panels show the soft color (ratio of count rate in 6–10 keV and 3–6 keV) and the hard color (ratio of count rate in 10–40 keV and 3–10 keV) as a function of time. Right panel shows the hardness intensity diagram (HID) during the hypersoft (shown in black) and the very high (shown in red) state. Two separate structures in the HID of VHS at different count rates are due to the peak and dip phase count rates of the binary orbital motion in the presence of a data gap. To compare with the HID f. we put the HID of the FSXR (shown in blue). The relative position of the FSXR and the hypersoft state . but a new state (very high state) is found between them with the AstroSat observation that coincides with the jet line .

Spectral Analysis and Results:

To confirm the HPS to VHS transition as indicated by the model-independent approach, we separately fit SXT+LAXPC joint spectra in the energy range 0.6–70.0 keV extracted during the first 40 ks (HPS) and last 40 ks (VHS).

1.We use the **diskbb model** to fit the HPS emission. However, the disk is embedded in a plasma medium accreted from the companion.

2.The **bremsstrahlung** emission from the collision between the inflowing and outflowing plasma has been taken care of by the **bremss model.**

3.To account for the interstellar medium absorption and the local, partial absorption by the accreted wind and hot medium, we use **tbabs and pcfabs models**, respectively.

4.To account for this hard X-ray residual, we use the **power-law model in XSpec**. The Fe emission line and an absorption feature are modeled using a **Gauss and a gabs model**, respectively.

5.Bestfit parameters along with 1σ errors are provided:

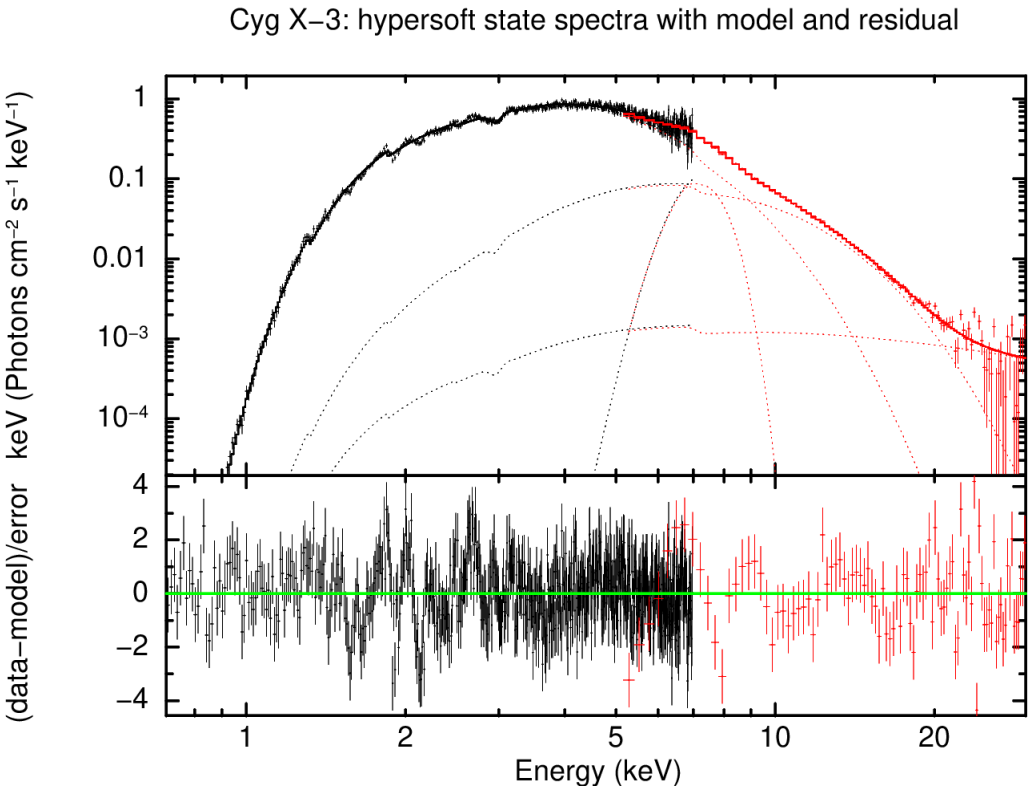

Hypersoft state fitted spectral parameters:

```
========================================================================
Model gabs<1>*pcfabs<2>*TBabs<3>*constant<4>(diskbb<5> + bremss<6> + nthComp<7> + gaussian<8>) Source No.: 1   Active/On
Model Model Component  Parameter  Unit     Value
 par  comp
                            Data group: 1
   1    1   gabs       LineE      keV      2.96030      +/-  9.87199E-03
   2    1   gabs       Sigma      keV      6.82973E-02  +/-  1.29869E-02
   3    1   gabs       Strength              4.10915E-02  +/-  5.20199E-03
   4    2   pcfabs     nH         10^22    15.8058      +/-  0.674385
   5    2   pcfabs     CvrFract              0.750444     +/-  2.23553E-02
   6    3   TBabs      nH         10^22    3.62330      +/-  5.68054E-02
   7    4   constant   factor                1.00000      frozen
   8    5   diskbb     Tin        keV      1.03504      +/-  5.66361E-02
   9    5   diskbb     norm                  1417.18      +/-  398.461
  10    6   bremss     kT         keV      35.9240      +/-  44.0844
  11    6   bremss     norm                  6.57258E-03  +/-  4.88216E-03
  12    7   nthComp    Gamma                 1.02496      +/-  0.646598
  13    7   nthComp    kT_e       keV      1.72090      frozen
  14    7   nthComp    kT_bb      keV      1.03504      = p8
  15    7   nthComp    inp_type   0/1      1.00000      frozen
  16    7   nthComp    Redshift              0.0          frozen
  17    7   nthComp    norm                  1.48379E-02  +/-  0.141347
  18    8   gaussian   LineE      keV      7.15784      +/-  6.66592E-02
  19    8   gaussian   Sigma      keV      0.668850     +/-  7.67592E-02
  20    8   gaussian   norm                  3.02138E-02  +/-  4.34559E-03
```

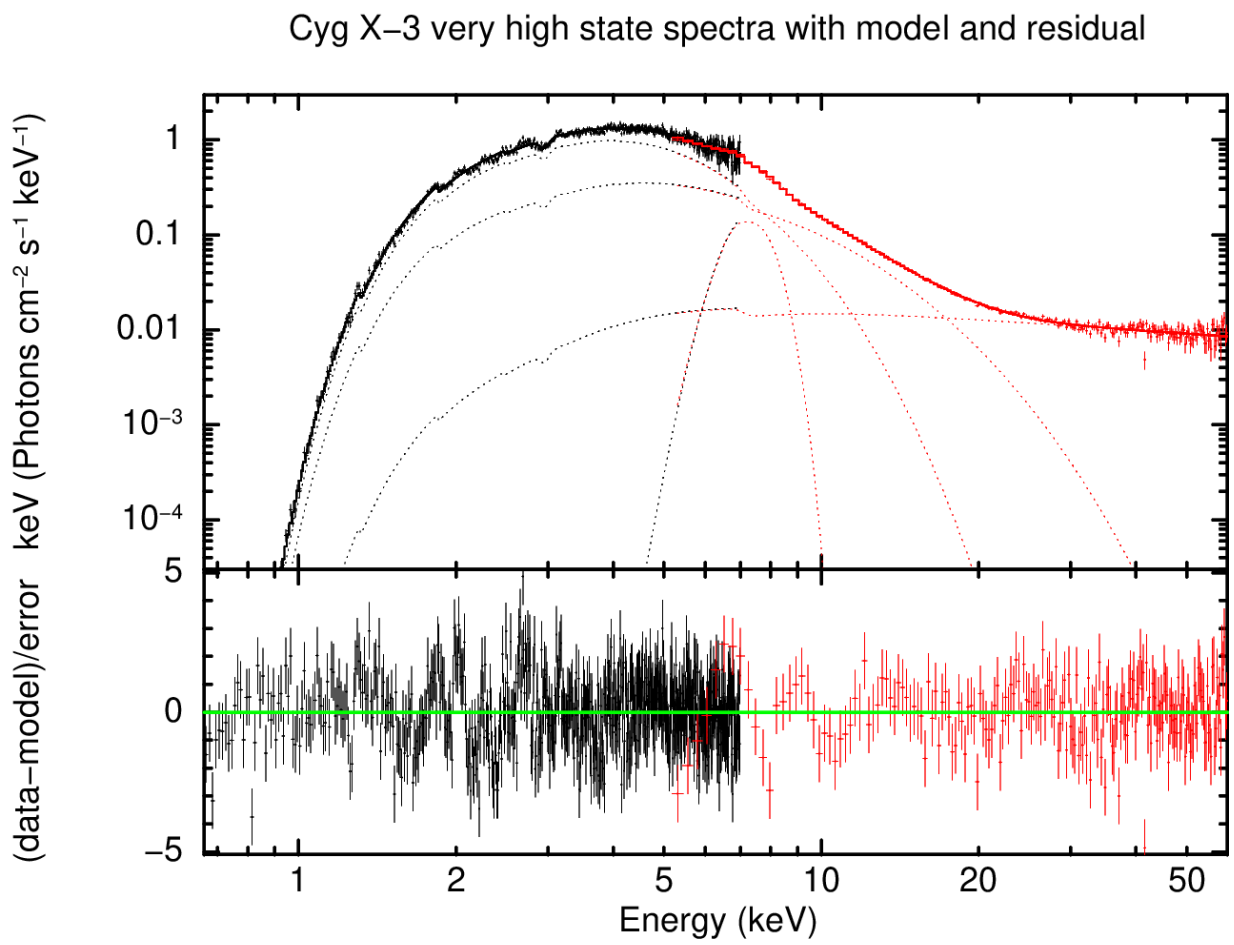

Very high state fitted spectral parameters:

```
========================================================================
Model gabs<1>*pcfabs<2>*TBabs<3>*constant<4>(diskbb<5> + bremss<6> + nthComp<7> + gaussian<8>) Source No.: 1   Active/On
Model Model Component  Parameter  Unit     Value
 par  comp
                            Data group: 1
   1    1   gabs       LineE      keV      2.95346      +/-  1.02924E-02
   2    1   gabs       Sigma      keV      5.82800E-02  +/-  1.39192E-02
   3    1   gabs       Strength            2.93737E-02  +/-  3.97859E-03
   4    2   pcfabs     nH         10^22    14.4870      +/-  0.555814
   5    2   pcfabs     CvrFract            0.696203     +/-  1.77293E-02
   6    3   TBabs      nH         10^22    3.70413      +/-  4.55483E-02
   7    4   constant   factor              1.00000      frozen
   8    5   diskbb     Tin        keV      1.10542      +/-  3.55080E-02
   9    5   diskbb     norm                1101.50      +/-  193.947
  10    6   bremss     kT         keV      3.85611      +/-  0.177720
  11    6   bremss     norm                3.51146      +/-  0.608189
  12    7   nthComp    Gamma               1.47045      +/-  3.53602E-02
  13    7   nthComp    kT_e       keV      1000.00      frozen
  14    7   nthComp    kT_bb      keV      1.10542      = p8
  15    7   nthComp    inp_type   0/1      1.00000      frozen
  16    7   nthComp    Redshift            0.0          frozen
  17    7   nthComp    norm                2.67003E-02  +/-  3.44383E-03
  18    8   gaussian   LineE      keV      7.23812      +/-  5.97528E-02
  19    8   gaussian   Sigma      keV      0.666903     +/-  7.48415E-02
  20    8   gaussian   norm                4.53224E-02  +/-  5.48857E-03
```

Summary and Conclusions:

1.In this work, we jointly analyze observations of Cyg X-3 using simultaneous SXT and LAXPC data on board AstroSat.

2.During the first half of the AstroSat observation (~0–50 ks), the X-ray spectra are unusually soft, and the source is not detected significantly above 20 keV.

3.. During the second half of the observation (~60–93 ks), the 20–60 keV count rate increases by a factor of ~5–6 and the hardness ratio also increases by ~50%.

4.We used hypersoft state (before radio jet) and very high state (during radio jet) spectra obtained first time by AstroSat for the Cyg X-3 source

5.Both spectra are fitted with a model consisting of a complex absorber, disk blackbody, thermal comptonisation and bremsstrahlung model.

6.We found that hypersoft state is dominated by the thermal blackbody emission

7.During the VHS, a flat X-ray power-law component (power-law index of ~1.47) appears in the high energy range (above 20 keV) of the spectra.

8.we note that during the HPS to the VHS transition, the inner disk temperature decreases from ~1.39 keV to ~1.11 keV, while the inner disk radius (which is proportional to the square root of diskbb normalization) increases by a factor of ~2. This implies the inner disk recedes during the formation of a major plasma blob that emits a radio flare

9. Comparing with the contemporary radio flux we conclude that such a flat X-ray power-law emission is solely due to the synchrotron emission from the slowly moving jet base.

10.Such a flat power-law is unusual and its origin may be the base of the Radio jet that emits synchrotron radiations.